Electronic Supplementary Material (ESI) for New Journal of Chemistry.
This journal is © The Royal Society of Chemistry and the Centre National de la Recherche Scientifique 2022

Supporting Information

A Combined Experimental and Theoretical Study on *p*-Sulfonatothiacalix[4]arene Encapsulated Sulisobenzone

Niloy Roy[a], Pranish Bomzan[a,b], Biswajit Ghosh[a], and Mahendra Nath Roy[*,a,c]

[a]Department of Chemistry, University of North Bengal, Darjeeling-734013, India

[a,b]Department of Chemistry, Gorubathan Government College, Kalimpong-735231, India

[c]Department of Chemistry, Alipurduar University, Alipurduar-736122, India

*Corresponding authors E-mail: *mahendraroy2002@yahoo.co.in*;
vcapduniversity@gmail.com

EXPERIMENTAL SECTION

Materials

Both sulisobenzone and p-sulfonatothiacalix[4]arene were procured from TCI Chemicals Pvt. Ltd (India). The chemicals were of analytical-reagent grade and used without further purification (Table S1). The purity of sulisobenzone and *p*-sulfonatothiacalix[4]arene were >98%. Doubly distilled water was used in all experiments.

2.2. Instruments

All the UV-visible titrations were carried out in Agilent 8453 UV-vis spectrophotometer with uncertainty ±2 nm where a quartz cell (1 cm×1 cm×4 cm) with a conventional 1 cm path length has been used.

The KBr disk technique was employed to record Fourier Transform Infrared (FTIR) spectra by Perkin Elmer spectrometer in the wavenumber range 4000-400 cm^{-1} with a 2 cm^{-1} resolution. The sample and KBr were taken in the ratio of 1:100 to prepare the disks.

Solution state ^1H NMR experiments were performed on Bruker Avance 300 MHz NMR spectrometer using D_2O as a solvent at 298.15 K. The residual D_2O peak was taken as an internal standard.

The mass characterization was performed using electrospray ionization mass spectrometer (ESI–MS) in positive mode with scan range 0-1200 m/z. The solution (90 : 10) water : methanol was thoroughly used with the flow being 0.120 ml/min.

All the DSC spectra were recorded using Perkin Elmer Pyris DSC 6. Heating of 1.2 mg of sample in all cases was carried out in the range of 30–300°C at a rate of 10°C/min under a N_2 gas flow of 40 mL/min.

2.3. Preparation of inclusion complex

The inclusion complex of SBZ and TSC4X was prepared using well-known co-precipitation method.[1] A mixed solution of TSC4X (30.8 mg, 4.0 mmol) and SBZ (90.5 mg, 4.0 mmol) in 1:1 molar ratio was prepared in 25 mL double distilled water. Then the mixed solution was stirred in a magnetic stirrer at 55℃ for 48 hrs till the emergence of a white precipitate. The white precipitate was filtered cautiously, and washed with ethanol followed by water for four times to eliminate uncomplexed SBZ and TSC4X. The resulting precipitate was then dried in a hot air oven at 50 °C for 12 hrs. The obtained inclusion complex was kept in a dessicator prior to analysis.

2.4. Preparation of 3D-structures of SBZ and TSC4X

The crystal structures of SBZ was collected from PubChem website (http://pubchem.ncbi.nlm.nih.gov). TSC4X was extracted from a complex with deposit number (CCDC ID : 246364) from Cambridge Crystal Data Centre (CCDC).[2] The missing hydrogen atoms and atomic charges were added to TSC4X as well as SBZ, and energy minimization was carried out with DFT-B3LYP method using Gaussian 09 software.[3] These structures were used to perform the computational studies.

2.5. Molecular docking evaluation

Molecular docking is a computational process for predicting the predominant binding mode of a guest with a host.[4] An established docking protocol for host-guest system implemented in PyRx was applied.[5] Before conducting docking, PDB files of SBZ and TSC4X were converted into PDBQT format, and atomic coordinates were generated using PyRx docking software. The grid box center values were set as center_x= 6.0424, center_y= 3.6790 and center_z= 17.4442, and dimension values as size_x= 19.2728, size_y = 17.8871 and size_z = 17.3422 for all three coordinates. The grid box size was adjusted on binding pocket of TSC4X (receptor) to sufficiently allow SBZ (ligand) to move freely in the search space. Based on docking score, the lowest energy docked conformer, as visualized by Discovery Studio Visualizer, v21.1.0.20298, BIOVIA,[6] was selected.

2.6. Aqueous solubility of SBZ-TSC4X complex

The aqueous solubility of SBZ-TSC4X complex was determined at 25°C.[7,8] Firstly, a sufficient quantity of SBZ-TSC4X complex was added to 5 ml water to ensure that the solution reached saturation. The solution at 25°C was shaken mechanically for 3 h. Secondly, the solution was filtered using 0.45 μm Nylon Cameo syringe filter to remove remaining solid from the solution. The solubility or saturated concentration of SBZ-TSC4X complex in water was then measured using UV-visible spectrophotometry.

Tables

Compound name	Molecular formula	Molecular weight	CAS number	Purity	Purchased from
Sulisobenzone (SBZ)	$C_{14}H_{12}O_6S$	308.30	4065-45-6	>98.0%	TCI Chemicals India
TSC4X	$C_{24}H_{12}Na_4O_{16}S_8$	904.78	211561-04-5	>98.0%	TCI Chemicals India

Table S1. Description of the materials purchased for the study

SBZ(ml)	TSC4X(ml)	SBZ (μM)	TSC4X (μM)	[SBZ]/ ([SBZ]+[TSC4X])	Absorbance(A)	ΔA	ΔA* [SBZ]/([SBZ]+[TSC4X])
0	4	0	100	0	0	0.6835698	0
0.4	3.6	10	90	0.1	0.51102745	0.17254235	0.017254235
0.8	3.2	20	80	0.2	0.53473523	0.14883457	0.029766914
1.2	2.8	30	70	0.3	0.55174562	0.13182418	0.039547254
1.6	2.4	40	60	0.4	0.57425983	0.10930997	0.043723988
2	2	50	50	0.5	0.59006421	0.09350559	0.046752795
2.4	1.6	60	40	0.6	0.61136452	0.07220528	0.043323168
2.8	1.2	70	30	0.7	0.62587152	0.05769828	0.040388796
3.2	0.8	80	20	0.8	0.64168432	0.04188548	0.033508384
3.6	0.4	90	10	0.9	0.66121687	0.02235293	0.020117637
4	0	100	0	1	0.6835698	0	0

Table S2. Data for the Job plot performed by UV-Visible spectroscopy for aqueous SBZ-TSC4X system at 298.15K

Temp/ (K)	[SBZ] (μM)	[TSC4X] (μM)	$A_\circ$	A	ΔA	1/[TSC4X] (M^{-1})	1/ΔA	Intercept	Slope	$K_a x10^{-3}$ (M^{-1})
	10	10	0.475814	0.501675	0.025861	100000	38.66794			
	10	20	0.475814	0.521454	0.045639	50000	21.91086			
	10	30	0.475814	0.540155	0.06434	33333.33	15.54232			
	10	40	0.475814	0.560025	0.084211	25000	11.87498			
298.15	10	50	0.475814	0.576114	0.1003	20000	9.970124	2.23508	0.000372	6010
	10	60	0.475814	0.596464	0.12065	16666.67	8.288444			
	10	70	0.475814	0.612545	0.13673	14285.71	7.313665			
	10	80	0.475814	0.626368	0.150554	12500	6.642151			

10	90	0.475814	0.644726	0.168912	11111.11	5.920238
10	100	0.475814	0.668851	0.193037	10000	5.180353

Table S3. Data for the Benesi-Hildebrand double reciprocal plot performed by UV-Vis spectroscopy for aqueous SBZ-TSC4X system at 298.15 K

SBZ	TSC4X	SBZ-TSC4X inclusion complex
1697 cm^{-1} : C=O stretching **1490, 1556 cm^{-1} :** aromatic C=C stretching **1265 cm^{-1} :** aromatic C-H bending **1073 cm^{-1} :** aliphatic C-O stretching **1208 cm^{-1} :** SO_3H stretching	**3353 cm^{-1} :** aromatic O-H stretching **1638, 1452 cm^{-1} :** aromatic skeletal C=C stretching vibrations **1210, 1046 cm^{-1} :** SO_3^- stretching vibrations	**1084 cm^{-1} :** aliphatic C-O stretching **1627, 1446 cm^{-1} :** aromatic skeletal C=C stretching

Table S4. FTIR data of pure SBZ, pure TSC4X and inclusion complex SBZ-TSC4X.

	protons	ppm (D_2O)			$\Delta\delta_{complex-SBZ} = \delta_{complex} - \delta_{SBZ}$	$\Delta\delta_{complex-TSC4X} = \delta_{complex} - \delta_{TSC4X}$
		δ_{SBZ}	δ_{TSC4X}	$\delta_{complex}$		
SBZ	H-1	6.45 (1H, s)		6.45 (1H, s)	0.00	
	H-2	6.70-6.72 (1H, d, J= 8Hz)		6.71-6.73 (1H, d, J=8Hz)	0.01	
	H-3	3.90 (3H, s)		3.90 (3H, s)	0.00	
	H-4	7.74-7.76 (2H, dd, J= 8Hz)		7.74-7.70 (2H, dd, J=16Hz)	-0.04	
	H-5	7.64-7.68 (2H, dd, J=16Hz)		7.64-7.60 (2H, dd, J=16Hz)	-0.04	
	H-6	7.48-7.52 (m)		7.48-7.52 (m)	-0.00	
TSC4X	Ar—O**H**		3.52 (4H, s)	3.53 (4H, s)		0.01
	Ar—**H**		7.78 (8H, s)	7.80 (8H, s)		0.02

Table S5. ^{1}H NMR data for SBZ and SBZ-TSC4X complex in D_2O.

Name of the complexes	Calculated mass (a.u)	Experimental mass (a.u)
$[SBZ\text{-}TSC4X+H]^+$	1214.08	1214.13
$[SBZ\text{-}TSC4X+Na]^+$	1236.08	1236.19

Table S6. ESI-MS analysis of the complexes with calculated as well as experimental mass.

Ligand with receptor	Binding affinity(ΔG) in kcal mol^{-1}
SBZ-TSC4X	-4.4

Table S7. Binding affinity of SBZ-TSC4X in different pose obtained from Molecular Docking.

Figures

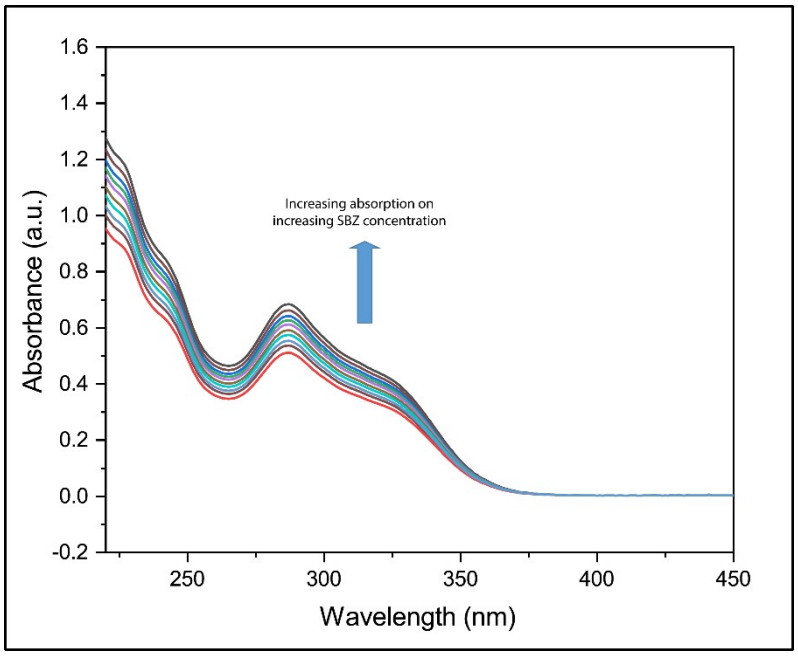

Figure S1. UV-visible absorption spectra of SBZ by varying both host and guest concentrations such that the sum of the concentrations of both components was kept constant ([SBZ]+[TSC4X] = 1.0×10^{-4} M).

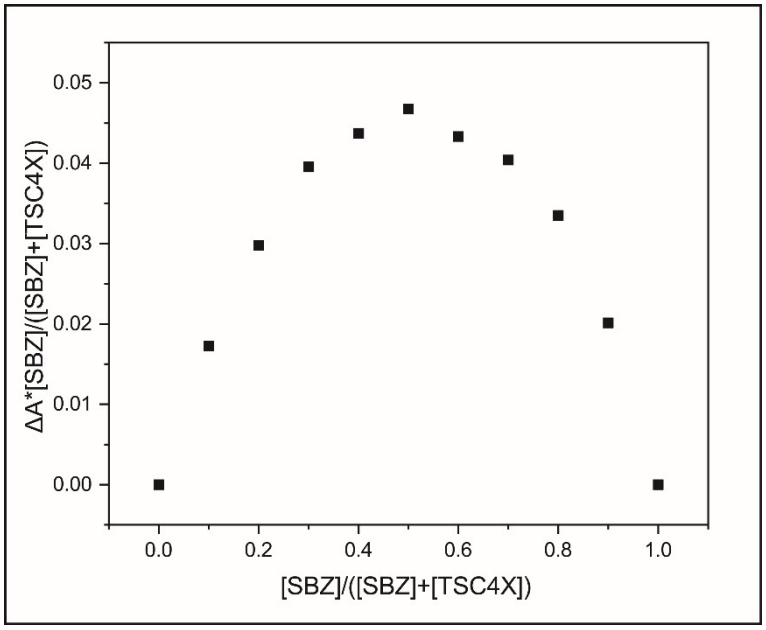

Figure S2. Job's plot of SBZ-TSC4X system at 298.15 K (λ_{max} = 287 nm).

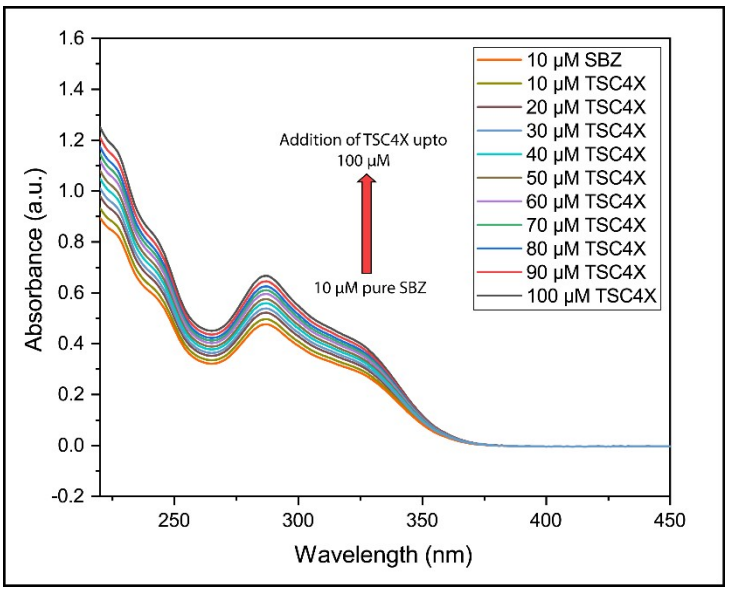

Figure S3. UV absorption spectra of SBZ in the absence and presence of various concentrations of TSC4X at 298.15 K; where, initial concentration of SBZ was 10 µM and variations of concentration of TSC4X started from 10 µM, 20 µM, 30 µM upto 100 µM.

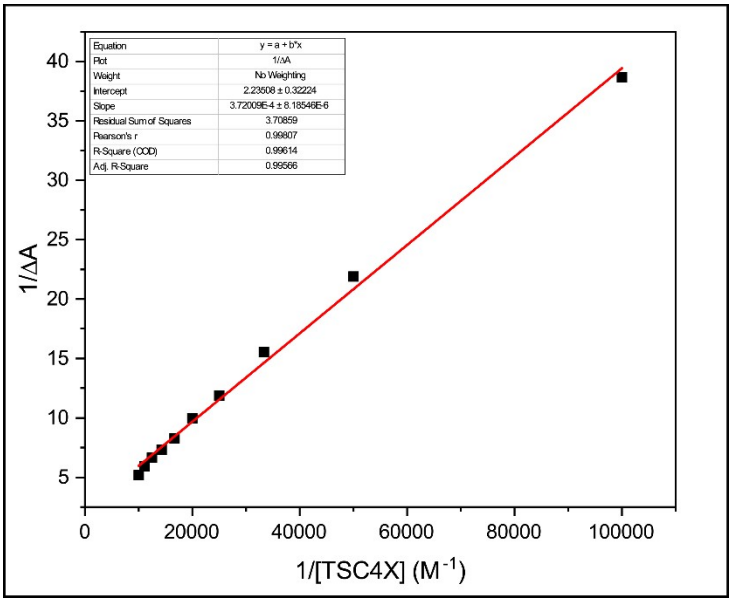

Figure S4. Double reciprocal Benesi-Hildebrand plot of 1/ΔA versus 1/[TSC4X] at 298.15 K.

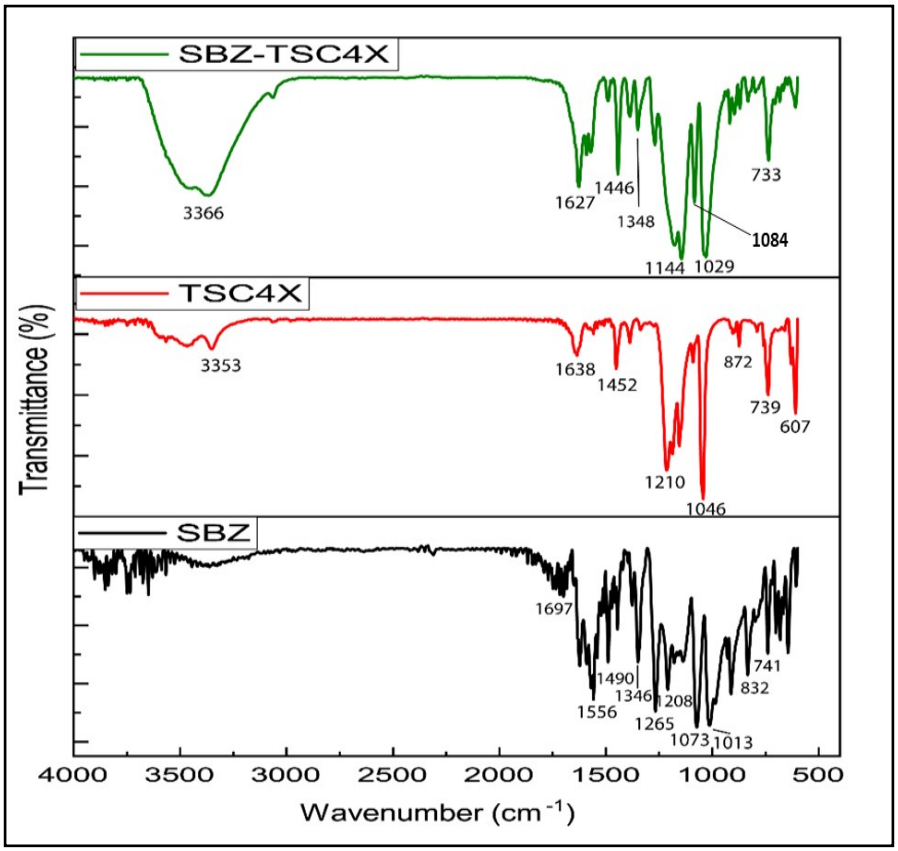

Figure S5. FT-IR spectra of **(a)** SBZ, **(b)** TSC4X and **(c)** SBZ-TSC4X inclusion complex.

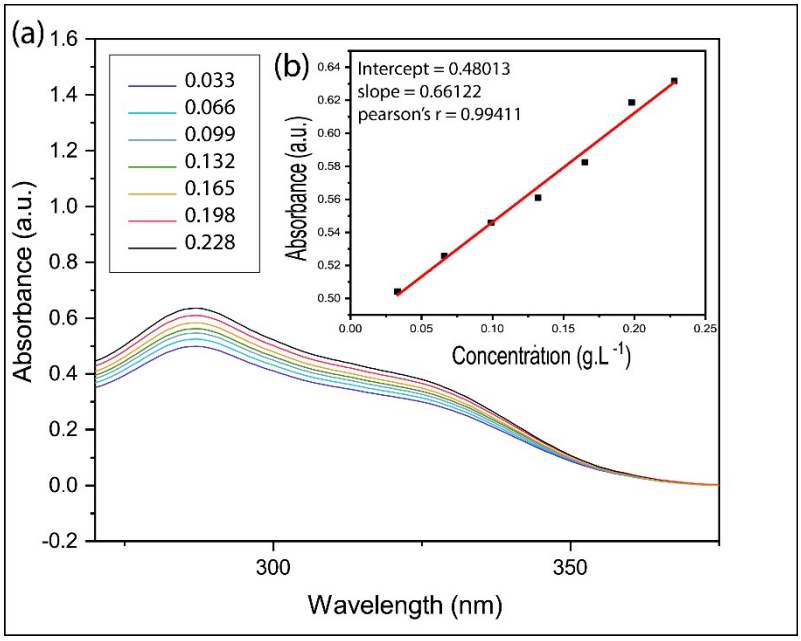

Figure S6. (a) UV-visible spectra of SBZ-TSC4X complex with different concentrations (g L^{-1}) in aqueous solution (pH = 7.0, 25°C). **(b)** A plot of absorbance of SBZ-TSC4X at 287 nm versus the concentration of SBZ-TSC4X complex.

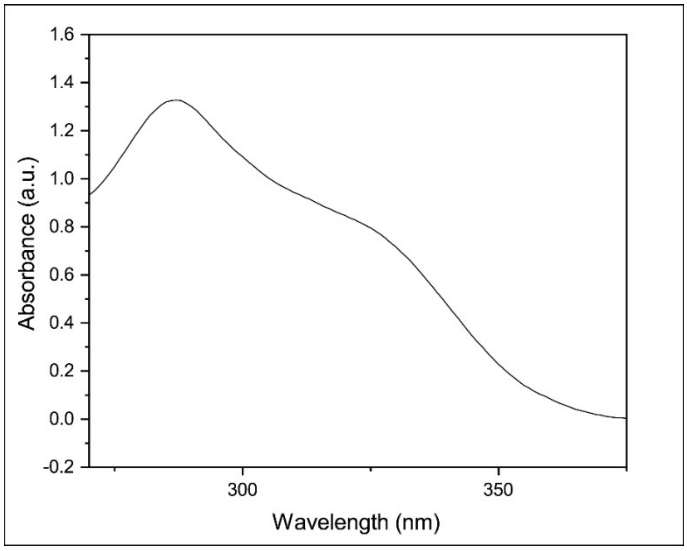

Figure S7. UV-visible spectra of SBZ-TSC4X saturated aqueous solution.

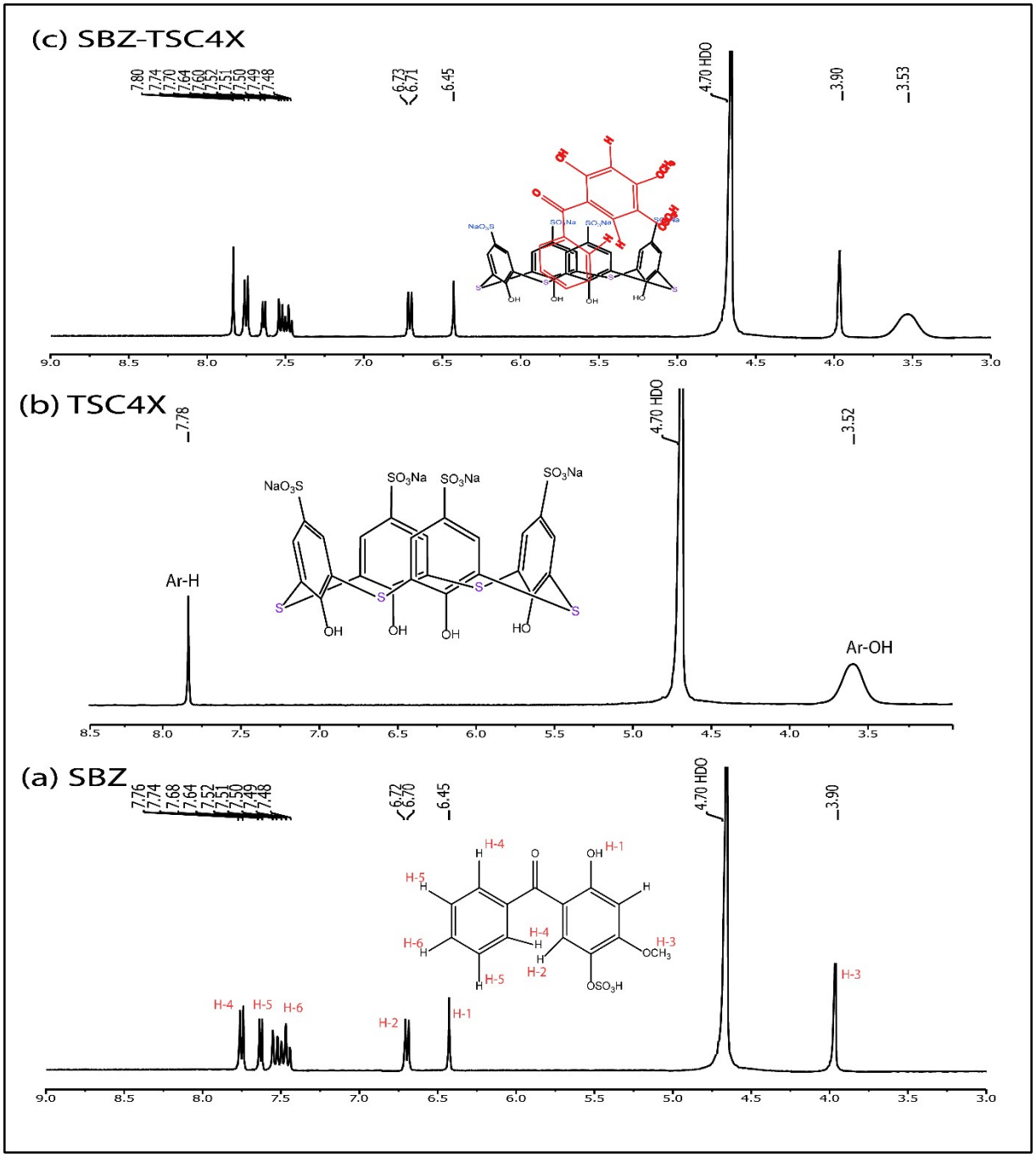

Figure S8. ^{1}H NMR spectra of **(a)** SBZ **(b)** TSC4X **(c)** SBZ-TSC4X inclusion complex.

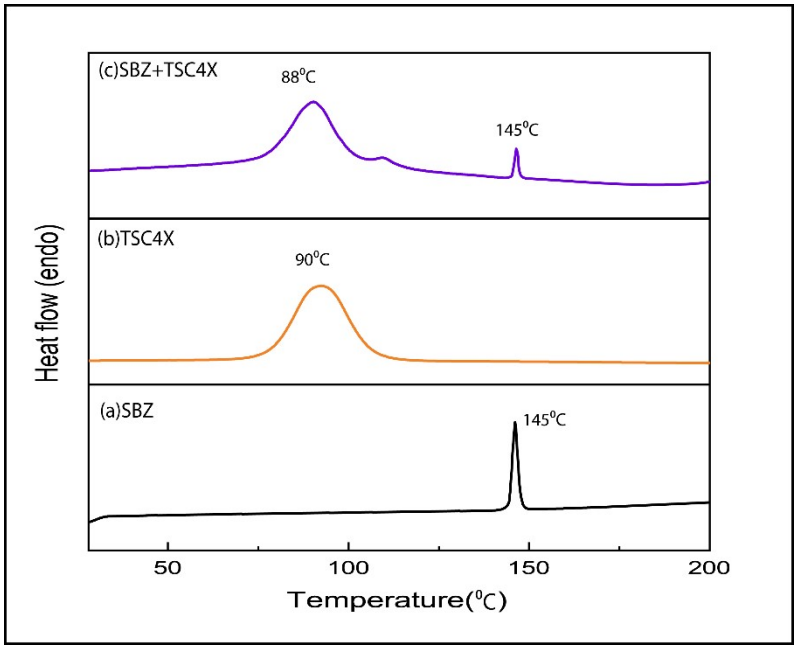

Figure S9. DSC thermograms of **(a)** SBZ **(b)** TSC4X **(c)** SBZ-TSC4X inclusion complex.

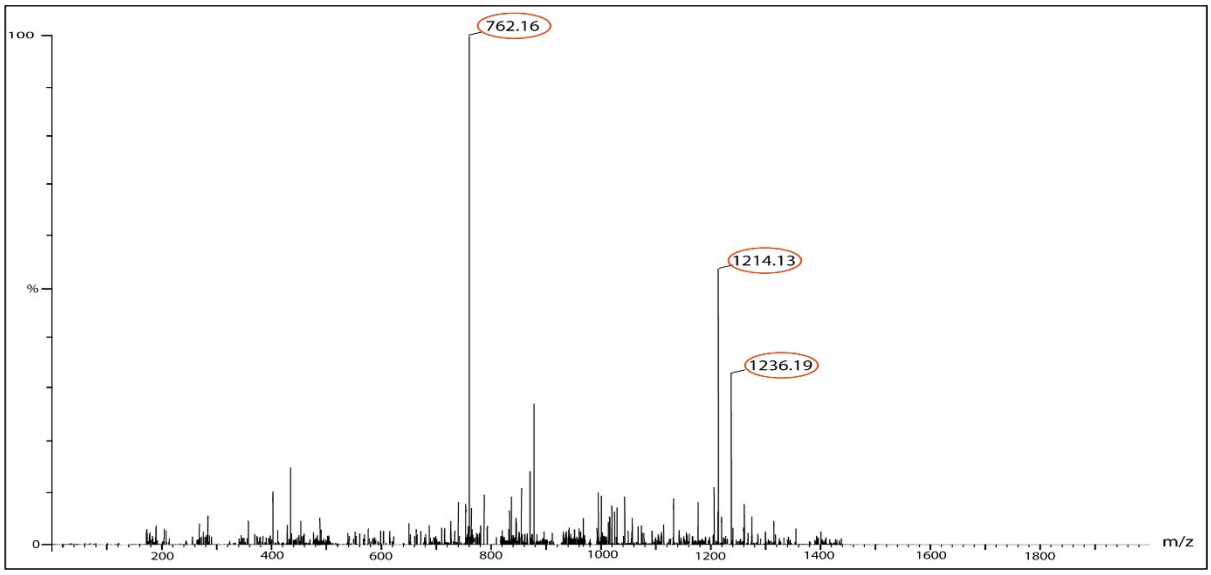

Figure S10. ESI mass spectra of SBZ-TSC4X inclusion complex.

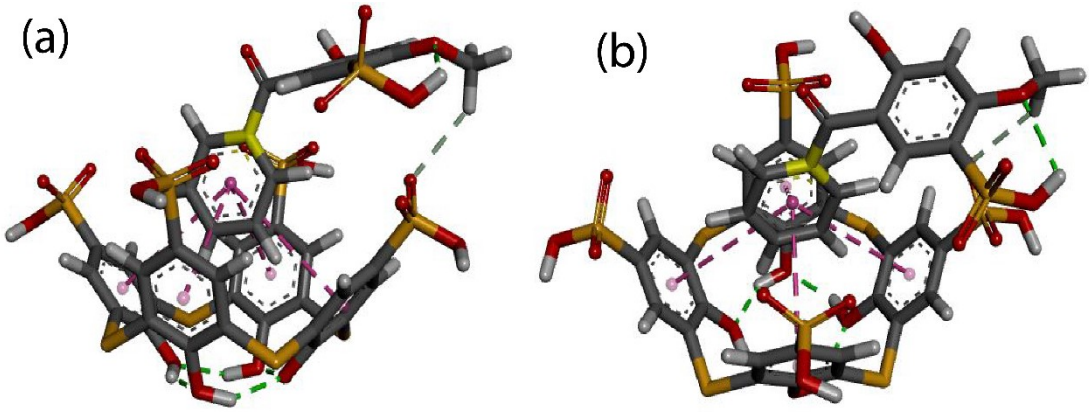

Figure S11. Best conformational model of SBZ-TSC4X inclusion complex, side view **(a)** and top view **(b).**

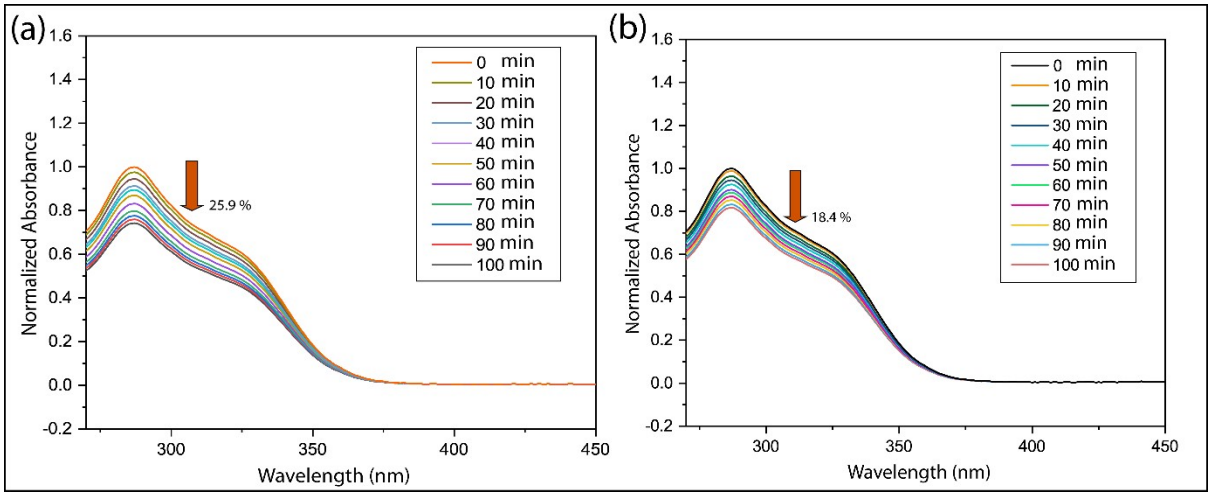

Figure S12. Absorption spectra of (a) SBZ and (b) SBZ-TSC4X complex recorded at different time intervals during UV irradiation.

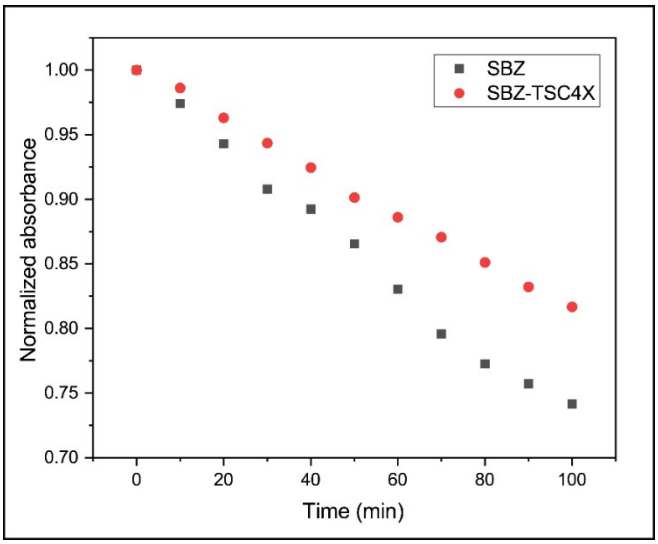

Figure S13. Normalized absorbance change over a period of time in minutes.

References

[1] H. Wu, H. Liang, Q. Yuan, T. Wang, X. Yan, *Carbohydr. Polym.* **2010**, *82*, 613-617.

[2] Y. Liu, D.S. Guo, E.C. Yang, H.Y. Zhang, Y.L. Zhao, *Eur*. *J*. *Org*. *Chem*. **2005**, *1*, 162-170.

[3] M. J. Frisch, G. W. Trucks, H. B. Schlegel, G. E. Scuseria, M. A. Robb, J. R. Cheeseman, G. Scalmani, V. Barone, G. A. Petersson, H. Nakatsuji, X. Li, M. Caricato, A. Marenich, J. Bloino, B. G. Janesko, R. Gomperts, B. Mennucci, H. P. Hratchian, J. V. Ortiz, A. F. Izmaylov, J. L. Sonnenberg, D. Williams-Young, F. Ding, F. Lipparini, F. Egidi, J. Goings, B. Peng, A. Petrone, T. Henderson, D. Ranasinghe, V. G. Zakrzewski, J. Gao, N. Rega, G. Zheng, W. Liang, M. Hada, M. Ehara, K. Toyota, R. Fukuda, J. Hasegawa, M. Ishida, T. Nakajima, Y. Honda, O. Kitao, H. Nakai, T. Vreven, K. Throssell, J. A. Montgomery, Jr., J. E. Peralta, F. Ogliaro, M. Bearpark, J. J. Heyd, E. Brothers, K. N. Kudin, V. N. Staroverov, T. Keith, R. Kobayashi, J. Normand, K. Raghavachari, A. Rendell, J. C. Burant, S. S. Iyengar, J. Tomasi, M. Cossi, J. M. Millam, M. Klene, C. Adamo, R. Cammi, J. W. Ochterski, R. L. Martin, K. Morokuma, O. Farkas, J. B. Foresman, and D. J. Fox, *Gaussian 09, Revision D.01*, Gaussian, Inc., Wallingford CT, **2016**.

[4] B. Ghosh, N. Roy, D. Roy, S. Mandal, S. Ali, P. Bomzan, K. Roy, M.N. Roy, *J. Mol. Liq.* **2021**, *344*, 117977.

[5] S. Dallakyan, A.J. Olson, *Chem. Biol*. **2015**, 243-250.

[6] BIOVIA, Dassault Systèmes, [Discovery Studio Visualizer], [v21.1.0.20298], San Diego: Dassault Systèmes, **2020**.

[7] W. Zhang, X. Gong, Y. Cai, C. Zhang, X. Yu, J. Fan, G. Diao, *Carbohydr. Polym.* **2013**, *95*, 366-370.

[8] W. Zhang, M. Chen, G. Diao, *Electrochimica Acta* **2011**, *56*, 5129–5136.